

# Structure of $\alpha$ -polypivalolactone: a refinement based on the Rietveld method

S. Brückner and S. V. Meille

Dipartimento di Chimica del Politecnico di Milano, Piazza Leonardo da Vinci 32,  
20133 Milano, Italy

and W. Porzio

Istituto di Chimica delle Macromolecole del CNR, Via E. Bassini 15, 20133 Milano, Italy  
(Received 8 October 1987; accepted 18 February 1988)

A comparative study is carried out on the structure of the  $\alpha$  form of polypivalolactone obtained (i) from the analysis of oriented-fibre X-ray diffraction diagrams, (ii) from conformational energy calculations and (iii) by refining the first two models through best fitting on the powder X-ray diffraction profile according to the Rietveld method. A single refined model is obtained that shows very good agreement both with experimental fibre intensities and with the powder profile. This result is discussed in terms of the accuracy of structural parameters derived from the Rietveld method compared with the much more numerous determinations based on X-ray diffraction from oriented samples.

(Keywords:  $\alpha$ -polypivalolactone; X-ray diffraction; Rietveld method)

## INTRODUCTION

The rapidly increasing number of crystal structure determinations or refinements through best fitting of X-ray powder diffraction profiles testifies to the present interest in this structural approach<sup>1-3</sup>. When polymers are involved, this method, known as the Rietveld whole-fitting method<sup>4</sup>, is particularly useful if oriented samples are not available; otherwise the analysis of diffraction diagrams from oriented fibres gives, in principle, more information. From a practical point of view, however, the latter statement does not appear always to be true. In fact, the one-dimensional distribution of diffracted intensities present in a powder profile, with consequent overlap problems, is compensated by the accuracy of intensity measurements. Moreover, diffracted intensities are compared as such with the calculated ones without the need for previous integration, which usually requires a number of subjective assumptions and is therefore the main source of systematic errors affecting the observed data. To be fair, however, we should point out that a powder diagram too may contain contributions that can only be dealt with approximately: first, the preferred orientation of microcrystals and, secondly, in the case of polymers, the contribution due to the amorphous fraction of the sample.

The recent introduction of routines to handle two-dimensional scanning microdensitometer data is indeed an important contribution to reducing the need for approximations and subjective decisions in evaluating integrated intensities from fibre diffraction patterns<sup>5</sup>. This is achieved, however, at the cost of heavy computations on a large number of data points.

As an example of the application of the Rietveld method and as a contribution to the development of a more positive attitude towards the reliability of structural data obtained in this way compared with structural models obtained through analysis of X-ray diffraction

diagrams of oriented samples, we decided to study, in a comparative way, a number of well known crystalline polymers.

Polypivalolactone (PPVL) is a highly crystalline polymer that crystallizes in the  $\alpha$  form when cooled slowly from the melt. A  $\beta$  form is also known to result from stretching  $\alpha$ -PPVL, while a  $\gamma$  form can be obtained, together with  $\alpha$ -PPVL, by increasing the cooling rate from the melt<sup>6,7</sup>.

The most stable  $\alpha$  form was first studied by Carazzolo<sup>8</sup> and later by Perego *et al.*<sup>9</sup> through accurate analysis of X-ray diffraction diagrams from an oriented fibre. It gives rise to a very detailed powder profile up to high  $2\theta$  values (see Figure 1), so that it was considered a particularly favourable example on which to carry out a comparative study. An additional reason for interest in this polymer structure is the significant deviation of the ester bond from *trans* planarity ( $\approx 16^\circ$ ) found in the study of Perego *et al.*<sup>9</sup> and criticized by Cornibert *et al.*<sup>10</sup>, who proposed, on the basis of minimum conformational energy, a chain model that shows the same fibre repeat (6.02 Å) but keeps the ester bond rigorously planar. The differences

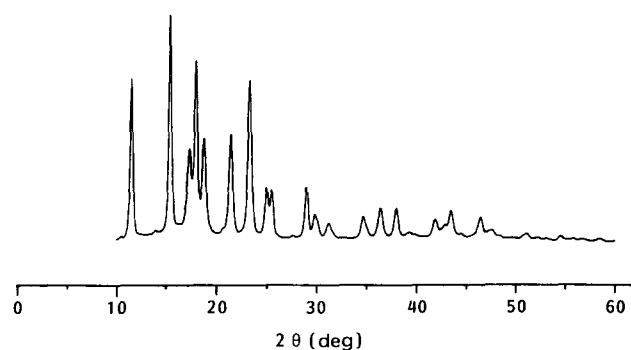


Figure 1 X-ray powder diffraction profile of PPVL

**Table 1** Experimental conditions of data recording

Instrument	Siemens D-500 goniometer equipped with step-scan attachment, proportional counter and Soller slits, controlled with a Hewlett-Packard computer
Radiation (power)	Cu K $\alpha$ , Ni-filtered (40 kV, 30 mA)
Divergence aperture (deg)	0.3
Receiving aperture (deg)	0.05
Step width (deg)	0.05 ( $2\theta$ )
Count time (seconds per step)	40
$2\theta$ range (deg)	10–60

between these two models are not dramatic but are large enough to give significant changes in the calculated profiles. We intend first to compare the structural model of Perego *et al.* (model I) and the model of Cornibert *et al.* (model II) with the observed powder profile of PPVL, and then to perform a refinement of both these models by the Rietveld method in order to see (i) whether a unique refined model (model III) can be obtained from different starting points and (ii) how this model would compare with previous structural data.

## EXPERIMENTAL

PPVL was prepared from pivalolactone as described in ref. 11, melted and subsequently annealed at 240°C for 1 h under an inert atmosphere. A powder was obtained by grinding the polymer and used to fill up the sample holder of a Siemens D-500 diffractometer. The main features of the data recording are reported in Table 1, while the collected X-ray powder diffraction profile is shown in Figure 1.

## STRUCTURAL ANALYSIS

The best-fitting program used throughout our analysis was originally written by Immirzi<sup>12</sup> and subsequently modified by one of the present authors to allow for the insertion of constraints among the generalized coordinates, in the form of Lagrange multipliers. Cell dimensions and the space group (monoclinic  $P2_1/c$ ) were taken from published data<sup>9</sup>, and only in the final optimization cycles did we let the cell parameters vary; only very modest changes took place.

Best fitting with the observed profile was achieved, in the case of model I, by refining all the following non-structural parameters: (i) the background contribution (in the form of a segmented line, where the intensities at the selected nodes are adjustable quantities); (ii) the peak widths at half-height and their  $2\theta$  dependence; (iii) the effect of preferred uniaxial orientation of crystallites; (iv) an overall scale factor between calculated and observed data; and (v) a zero correction to the experimental  $2\theta$  scale. Peak profiles were always calculated analytically in the form of Cauchy functions<sup>13</sup> and  $K\alpha_1$ – $K\alpha_2$  splitting was taken into account. The case of model II was more complicated because it is a theoretical model expressed through a set of atomic coordinates in an orthogonal system with  $z$  as the helix axis. Therefore, in addition to the aforesaid non-structural parameters, we also had to adjust the position of the chain within the unit cell. Coincidence of the helix axis with a crystallographic

binary screw axis reduced the number of adjustable structural parameters to 2, i.e. a rigid-body rotation and a translation around and along the helix axis. Furthermore, it was also necessary to generate the positions of hydrogen atoms, since they are absent in the original model II.

Results are shown in Figure 2, where profile A is the experimental profile and B and C represent the calculated profiles for models I and II, respectively. The overall disagreement factors for the two models, in terms of  $R = \sum |I_0 - I_c| / \sum I_{net}$  where  $I_{net} = I_0 - I_{backgr}$ , are 0.19 and 0.28 (0.33 without hydrogens) for models I and II, respectively. It is interesting to observe that, by decomposing these overall values into, roughly speaking, low-angle ( $2\theta \leq 30^\circ$ ) and high-angle ( $2\theta > 30^\circ$ ) contributions, we obtain a rather well balanced situation for model I ( $R_L = 0.18$ ,  $R_H = 0.21$ ), while model II shows a noticeable discrepancy ( $R_L = 0.24$ ,  $R_H = 0.38$ ) with poor agreement at high  $2\theta$  values.

In the final refinement cycles, the weight attributed to the peak at the lowest  $2\theta$  value ( $2\theta = 11.5^\circ$ ) was reduced to 0.1w. The intensity of this peak is in fact substantially reproduced by both models but, owing to the low absorption of the material, it is affected by appreciable aberrations that produce a marked asymmetry<sup>14</sup>, so that accurate fitting of the peak shape is difficult.

Model I was chosen first as the starting point for a refinement procedure also involving the chain geometry. In particular, all four torsion angles were allowed to vary, together with the valence angles. The repeat distance along the chain axis was kept constant throughout the calculations by the introduction of constraints on one bond length and two valence angles involving atoms that belong to adjacent unit cells. The refined model (model III) shows very good agreement with the observed profile, with an overall disagreement factor  $R = 0.135$  ( $R_L = 0.136$ ,  $R_H = 0.132$ ). A second refinement procedure was also carried out starting from model II to see whether a different, and worse, starting point might affect the final geometry, but this was not the case since the two refined models are indistinguishable. In this case, too, a reduced weight (0.1w) was attributed to the peak at the lowest  $2\theta$  value.

Results are shown in Figure 3, where profile A is the observed profile, B is the profile calculated with model III, C is the difference profile and the broken curve indicates

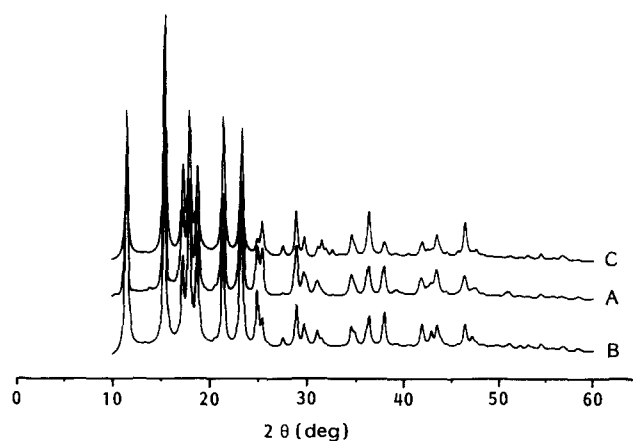


**Figure 2** A comparison of observed (A) and calculated powder profiles of PPVL. Profile B is calculated with model I, profile C with model II

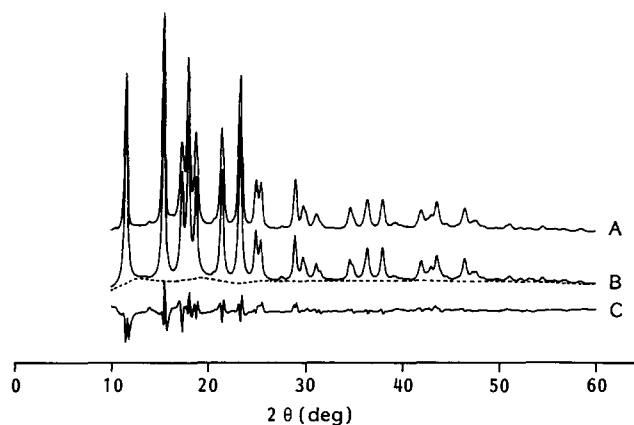


**Figure 3** The observed (A) powder profile of PPVL compared with the profile calculated with model III (B). Curve C is the difference profile and the broken curve is the calculated background contribution

**Table 2** Refined non-structural parameters

Zero correction ( $2\theta$ )(deg)	-0.033(4)
Profile function parameters <sup>a</sup>	
U	0
V	0.121(30)
W	0.082(6)
m	1
Intensities ( <i>k</i> counts) at the points on the segmented line	
$2\theta$ (deg)	Intensity
10	0.025(9)
13	0.104(4)
16	0.082(4)
20	0.114(4)
27	0.083(3)
35	0.080(2)
60	0.047(1)

<sup>a</sup> Peak shapes are calculated analytically through a Pearson VII function:

$$f(z) = (C/H_k)[1 + 4(2^{1/m} - 1)z^2]^{-m}$$

with

$$z = (2\theta_i - 2\theta_k)/H_k$$

and

$$H_k^2 = U \tan^2 \theta_k + V \tan \theta_k + W$$

$m = 1$  determines a peak profile following a Cauchy distribution

the background contribution. In Table 2 refined non-structural parameters are listed, in Table 3 we report the set of refined crystallographic coordinates and in Table 4 the chain geometry is described in terms of bond lengths, angles and torsion angles. In Figure 4 a view of the PPVL chain, orthogonal to the helix axis, is shown, along with the numbering scheme.

## DISCUSSION

The strong link with experimental data of model I as well as the theoretical nature of model II result quite clearly by inspection of Figure 2. The striking disagreement of model II at high angles ( $R_H = 0.38$ ) suggests that, while the overall model is, broadly speaking, correct, it fails just at the higher resolution required to specify local geometries in a precise way. The validity of force-field calculations is obviously not questioned here but, if high accuracy is invoked, it would be advisable to take into account

packing forces as well, particularly when polar groups are involved.

In Figure 5 we show a comparison of the main-chain torsion angles of models I, II and III. The two models refined on experimental data are in substantial agreement with regard to the main features of the conformation, i.e. the deviation from *trans* planarity of the ester bond ( $196^\circ$

**Table 3** Refined cell constants and final fractional coordinates of model III. Isotropic thermal factors for non-hydrogen atoms are  $B = 3.0 \text{ \AA}^2$

	x	y	z
O(1)	0.0198	0.6136	0.2704
O(2)	0.2285	0.4956	0.4814
C(1)	0.0691	0.2196	0.1711
C(2)	0.2211	0.3566	0.2792
C(3)	0.1607	0.4937	0.3581
C(4)	0.3686	0.1993	0.3764
C(5)	0.2881	0.5136	0.2116
H(1,1)	0.1167	0.0949	0.1314
H(1,2)	-0.0198	0.3269	0.0894
H(4,1)	0.3871	0.6225	0.2880
H(4,2)	0.3435	0.4144	0.1646
H(4,3)	0.1800	0.6124	0.1353
H(5,1)	0.3256	0.1029	0.4331
H(5,2)	0.4821	0.2982	0.4452
H(5,3)	0.3999	0.0882	0.3180

$a = 9.03(1) \text{ \AA}$ ,  $b = 6.01(1) \text{ \AA}$ ,  $c = 11.62(1) \text{ \AA}$ ,  $\beta = 121.5(1) \text{ deg}$ , space group  $P2_1/c$

**Table 4** Chain geometry of model III

<b>Bond lengths (Å)</b>			
C(1)-C(2)	1.53	O(1)-C(1)'	1.44
C(2)-C(3)	1.53	O(1)-C(3)	1.35
C(2)-C(4)	1.54	O(2)-C(3)	1.23
C(2)-C(5)	1.54		
<b>Bond angles (deg)</b>			
O(1)'-C(1)-C(2)	109.4	C(2)-C(3)-O(1)	109.0(5)
C(1)-C(2)-C(3)	109.5(5)	C(2)-C(3)-O(2)	125.9(5)
C(1)-C(2)-C(4)	109.5	C(3)-O(1)-C(1)'	114.6
C(1)-C(2)-C(5)	109.5		
<b>Torsion angles (deg)</b>			
O(1)'-C(1)-C(2)-C(3)	46.2(9)		
C(1)-C(2)-C(3)-O(1)	53.5(8)		
C(2)-C(3)-O(1)-C(1)'	190.6(9)		
C(3)-O(1)-C(1)'-C(2)'	182.2(8)		

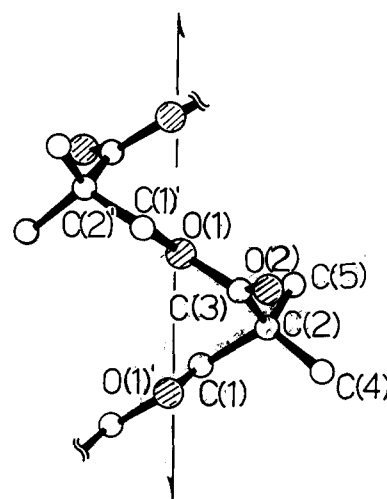


**Figure 4** A view of PPVL orthogonal to the helix axis. The numbering scheme is also indicated

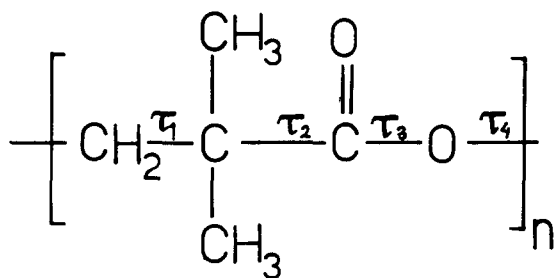


Figure 5 A comparison of the main-chain torsion angles for the three models (I, II, III) studied

	Torsion angle (deg)		
	I	II	III
$\tau_1$	41	60	46
$\tau_2$	61	34	54
$\tau_3$	196	180	191
$\tau_4$	178	208	182

and  $191^\circ$  for models I and III, respectively) and the deviation from a perfect *gauche* conformation of the bond connecting the two aliphatic carbon atoms. The agreement of the two models refined on X-ray data is a further<sup>15</sup> encouraging, though partial, answer to the question concerning the reliability of structural models derived from X-ray powder diffraction profiles. Furthermore, it is worth while pointing out that model III, refined on the observed powder profile, was also tested against intensity data obtained from the oriented fibre and published in the paper of Perego *et al.*<sup>9</sup>, giving rise to a disagreement factor  $R = \sum |I_0 - I_c| / \sum I_0$  of 0.15, equal to that of model I. This observation is not so obvious; in fact it is not uncommon that procedures and assumptions adopted for evaluating integrated intensities of X-rays diffracted by oriented fibres give results that are in poor agreement with powder spectra, and therefore it happens that a model showing the best agreement with one data set is not the best when compared with data

collected in a different way<sup>15</sup>. This was not the case here, and model III emerges as more likely than model I, not only in view of good agreement with a wider data set, but also because geometrical deviations from model I would produce a less strained geometry, i.e. the torsion angles of model III are closer than those of model I to the values of minimum conformational energy calculated in model II (see Figure 5).

In conclusion we believe the fibre and the powder methods to be substantially complementary rather than competitive in X-ray diffraction studies on polymers. The comparison carried out here indicates that, when high crystallinity and good peak resolution exist, the powder profile refinement is not to be considered just a secondary approach for crystal structure analysis.

## REFERENCES

- 1 Young, R. A. Main Lecture at the 13th Int. Congr. of Crystallography, Hamburg, 1984, and Collected Abstracts in section on 'Advances in Powder Diffraction'
- 2 Brückner, S., Di Silvestro, G. and Porzio, W. *Macromolecules* 1986, **19**, 235
- 3 Brückner, S., Luzzati, S., Porzio, W. and Sozzani, P. *Macromolecules* 1987, **20**, 585
- 4 Rietveld, H. M. *J. Appl. Crystallogr.* 1969, **2**, 65
- 5 French, A. D. and Gardner, K. H. (Eds.) 'Fiber Diffraction Methods', ACS Symp. Ser. 141, American Chemical Society, Washington DC, 1980; Symp. on Polymer Diffraction, Philadelphia, 1984: *J. Macromol. Sci.-Phys. (B)* 1985-86, **24**, 1-4.
- 6 Prud'homme, E. R. and Marchessault, R. H. *Macromolecules* 1974, **7**, 541
- 7 Meille, S. V., Konishi, T. and Geil, P. H. *Polymer* 1984, **25**, 775
- 8 Carazzolo, G. *Chem. Ind.* 1964, **46**, 525
- 9 Perego, G., Melis, A. and Cesari, M. *Makromol. Chem.* 1972, **157**, 269
- 10 Cornibert, J., Hien, N. V., Brisse, F. and Marchessault, R. H. *Can. J. Chem.* 1974, **52**, 3742
- 11 Borri, C., Brückner, S., Crescenzi, V., Della Fortuna, G., Mariano, A. and Scarazzato, P. *Eur. Polym. J.* 1971, **7**, 1515
- 12 Immirzi, A. *Acta Crystallogr. (B)* 1980, **36**, 2378
- 13 Hall, M. M., Jr *J. Appl. Crystallogr.* 1977, **10**, 66
- 14 Klug, H. P. and Alexander, L. E. 'X-ray Diffraction Procedures', Wiley, New York, 1974
- 15 Brückner, S., Meille, S. V., Malpezzi, L., Cesàro, A., Navarini, L. and Tombolini, R. *Macromolecules* 1988, **21**, 967